

Letter

Sputtered SnO₂/ZnO Heterostructures for Improved NO₂ Gas Sensing Properties

Bharat Sharma ^{1,*} , Ashutosh Sharma ² , Monika Joshi ³ and Jae-ha Myung ^{1,*}¹ Department of Materials Science and Engineering, Incheon National University, Incheon 22012, Korea² Department of Materials Science and Engineering and Department of Energy Systems Research, 206-Worldcup-ro, Yeongtong-gu, Suwon 16499, Gyeonggi-do, Korea; ashu@ajou.ac.kr³ Amity Institute of Nanotechnology, Amity University, Noida, Uttar Pradesh 201313, India; mjoshi@amity.edu

* Correspondence: bharatsharma796@gmail.com or b.sharma@inu.ac.kr (B.S.); mjaeha@inu.ac.kr (J.-h.M.)

Received: 5 July 2020; Accepted: 5 August 2020; Published: 7 August 2020



Abstract: A highly sensitive and selective NO₂ gas sensor dependent on SnO₂/ZnO heterostructures was fabricated using a sputtering process. The SnO₂/ZnO heterostructure thin film samples were characterized by field emission scanning electron microscopy (FESEM), X-ray diffraction (XRD), Energy-dispersive X-ray spectroscopy (EDS), and X-ray photoelectron spectroscopy (XPS). Sensors fabricated with heterostructures attained higher gas response ($S = 66.9$) and quicker response-recovery (20 s, 45 s) characteristics at 100 °C operating temperature towards 100 ppm NO₂ gas efficiently in comparison to sensors based on their mono-counterparts. The selectivity and stability of SnO₂/ZnO heterostructures were studied. The more desirable sensing mechanism of SnO₂/ZnO heterostructures towards NO₂ was described in detail.

Keywords: SnO₂/ZnO; heterostructures; NO₂ gas; MOS; sensing mechanism

1. Introduction

The effective detection of numerous harmful and toxic gases has become extremely vital for human health safety. Nitrogen oxide (NO₂), mostly released by fossil fuel combustion and motor vehicles, is one of the most hazardous air pollutants. It can cause various fatal diseases even at very low concentrations. Hence, the development of the NO₂ gas sensor is extremely important for health protection and environmental applications [1,2]. Metal oxide semiconductors (MOS) have been studied and utilized as effective and dominant methods in the detection of explosive or toxic gases and environmental monitoring [3,4]. Consequently, the variety of semiconductor metal oxides such as WO₃ [5], In₂O₃ [6], NiO [7], ZnO [8], and SnO₂ [2] with numerous morphologies have been studied for gas sensing applications to detect various gases that include reducing and oxidizing gases. In spite of all its advantages, the development of a highly selective gas sensor based on MOS is still a challenge [9]. The sensing characteristics of the MOS are dependent on its morphology, composition, and crystalline size.

To improve the selectivity and sensor response of MOS many approaches are utilized that includes the doping of the transition metal, loading of the noble metal catalyst, and developing binary metal oxides. Previously, several studies confirmed that the sensing materials consisting of two MOS exhibited better sensing characteristics than their mono counterparts [10]. Thus, many hybrid materials such as SnO₂/Fe₂O₃, CeO₂/ZnO, In₂O₃/ZnO, and SnO₂/ZnO with numerous morphologies have been considered for gas sensing applications and attained improved sensor response [11–14]. As the important gas sensing materials, SnO₂ and ZnO having band gaps of 3.6 eV and 3.4 eV, individually, previously reported for gas sensors. Recently, several studies have shown that sensing performance SnO₂ or ZnO can be highly enhanced by the formation of SnO₂/ZnO heterostructures [15].

In the present study, NO₂ gas response was highly enhanced by the use of the SnO₂/ZnO heterostructures synthesized by RF-sputtering. So far, SnO₂/ZnO heterostructures have been broadly studied to sense different oxidizing gases. The SnO₂/ZnO heterostructures were used to fabricate an NO₂ gas sensor, and gas sensing characteristics were studied by varying operating temperature and gas concentrations. The improvement in sensing performance may be credited to the formation of SnO₂/ZnO heterostructures.

2. Experimental

For the formation of gas sensors, an SiO₂-deposited silicon substrate was prepared with inter-digitated electrodes including that of a Pt (200 nm) layer that was coated on a sensor platform through the sputtering process. The deposition of thin-film SnO₂ and ZnO was done by utilizing RF-sputtering from SnO₂ and ZnO targets. The co-sputtering of the two targets was done at room temperature (RT). The base pressure inside the sputtering chamber was held around 5.5×10^{-6} mbar. The thin films were deposited at a O₂/Ar flow ratio of 50:50. The sputtering powers utilized for SnO₂ and ZnO were 50 and 80 W, respectively. The working pressure of the sputtering chamber was sustained at 9.0×10^{-3} mbar to attain oxide films. Lastly, heat treatments at 500 °C were done for 3 h in air to confirm the stability of the gas sensor. The morphological properties of the sensing film were characterized by utilizing FE-SEM and EDS that was combined with FE-SEM. The structural characteristics of the sensing film were examined through XRD using CuK_α X-radiation with a wavelength of 1.55178 Å and an analysis of surface elements was made by XPS.

The sensor characteristics were examined by using the flow-through technique that is described elsewhere [16]. In the gas sensing chamber, two tungsten wires were utilized for an electrical connection to the gas sensor. A sequences of mass flow controllers (MFCs) were utilized for maintaining the insertion of NO₂ gas inside the sensing chamber. Figure 1 shows the schematic for the gas sensing set-up along with the dimensions of the gas sensor. Initially, dry air was inserted inside until the saturation in the baseline sensor resistance was touched. The sensor electrical resistance was uninterruptedly noted by a Keithley multimeter (model 2600A) coupled to a laptop for continuously switching the NO₂ and dry air on and off through every cycle. The flow rate of gases was maintained around 200 sccm. Gas response is considered as $S = R_a/R_g$, where R_g and R_a are the electrical resistances in NO₂ gas and dry air, respectively. From this experiment, a gas concentration of 100 ppm NO₂ diluted nitrogen (N₂) and diluted with dry air as a carrier utilizing MFCs to attain a lower concentration. The concentration of the gas was premeditated as $\text{NO}_2 \text{ (ppm)} = \text{NO}_{2\text{std}} \text{ (ppm)} \times f/(f + F)$, where F and f are the flow rates of dry air and NO₂ gas, respectively. The selectivity of the sensor was measured with other interfering gases such as acetone, hydrogen, methanol, ammonia, and ethanol.

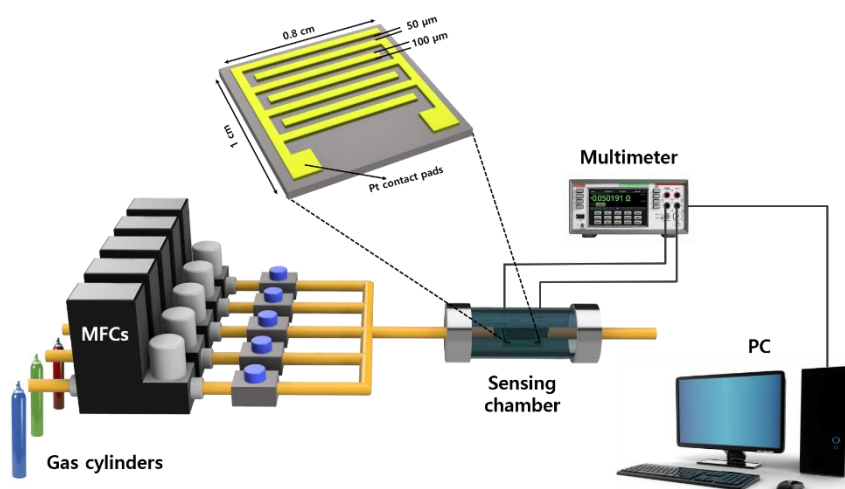


Figure 1. The schematic for gas sensing set-up along with dimensions of the gas sensor.

3. Results and Discussions

The surface morphology of the SnO₂/ZnO was examined by FESEM. Figure 2a displays the FESEM image of the thin film displayed uniformly distributed columnar microstructure, conforming to the zone structure model. Similar nanostructures were observed in another report and also in [17]. The thickness of SnO₂/ZnO thin film was around 10 nm, verified by cross-sectional view as shown in inset of Figure 2a. The elemental distribution of the SnO₂/ZnO thin film was studied by EDS analysis. Figure 2b–e shows EDS mapping of the SnO₂/ZnO thin film. The existence of Sn, Zn, and O elements validated the compositional purity of the deposited films.

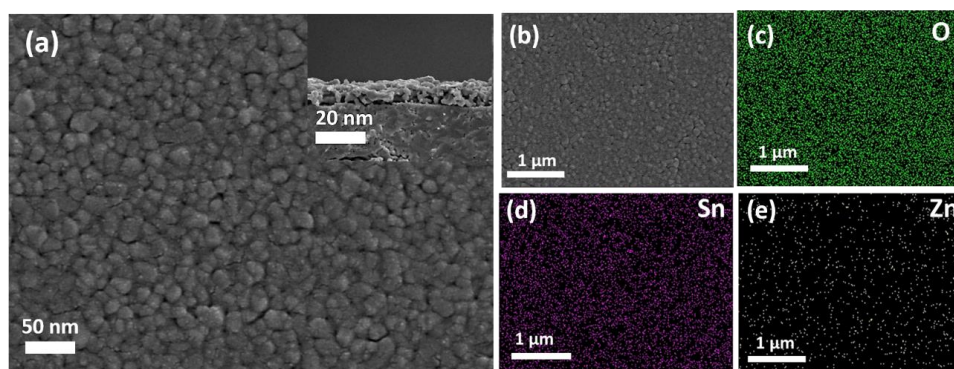


Figure 2. (a) FESEM for SnO₂/ZnO heterostructures (Inset: cross-section view), (b–e) EDS mapping with elements for O, Sn, and Zn.

The XRD pattern shows the crystallographic structure and phase purity of the SnO₂/ZnO thin film, as shown in Figure 3. The diffraction displayed sharp, clear, and strong diffraction peaks, that are well matched with the rutile-like structure of SnO₂ (JCPD # 41-1445) and hexagonal wurtzite phase of ZnO (JCPD # 36-1451), respectively [18]. Moreover, no impurity peaks were observed; that is a clear indication for the formation of SnO₂/ZnO heterostructures.

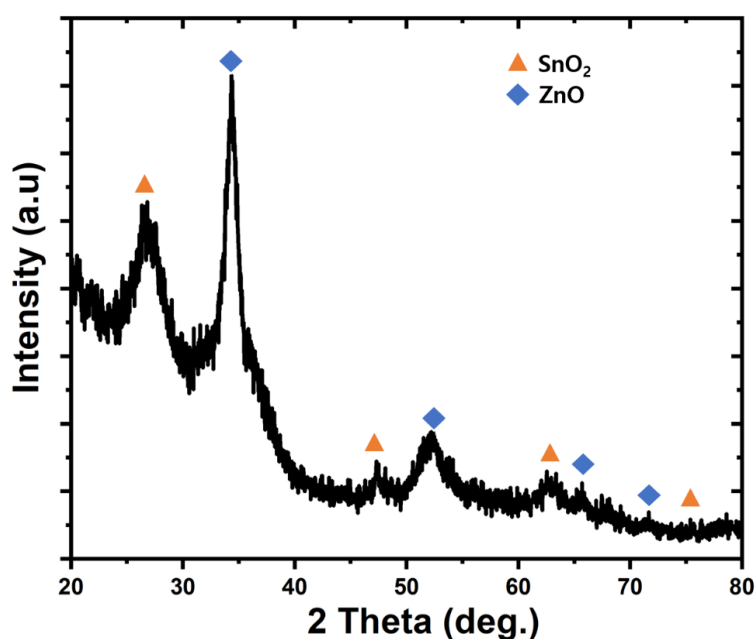


Figure 3. XRD patterns of SnO₂/ZnO heterostructures.

XPS study was done to inspect the chemical states of Sn and Zn and the surface composition in SnO₂/ZnO heterostructures. As presented in Figure 4a, the XPS survey spectrum indicates that

the SnO₂/ZnO heterostructures show the existence of Sn, Zn, and O elements. Figure 4b presented the high-resolution spectra for Sn 3d. Two peaks at binding energies 492.5 eV and 484 eV can be credited to the binding energies of Sn 3d_{3/2} and 3d_{5/2}, respectively, which are assigned Sn⁴⁺ cations [19]. The doublet peaks conforming to Zn 2p_{1/2} and Zn 2p_{3/2} were spotted, as shown in Figure 4c. The peak positions of Zn 2p_{1/2} and Zn 2p_{3/2} were situated at 1043.3 eV and 1020.5 eV, respectively, and the binding energy distance between Zn 2p_{1/2} and Zn 2p_{3/2} is 23.2 eV, signifying the Zn species were present in the chemical state Zn²⁺ [20]. The O 1s spectra is displayed in Figure 4d; the broad peak of O 1s is irregular and can be fitted into two peaks at 528.6 eV and 529.7 eV that corresponds to chemical states for O in the SnO₂/ZnO heterostructures. The peak at 528.6 eV binding energy corresponds to lattice oxygen denoted by O_I in Figure 4d, whereas the peak at 529.7 eV is related to the chemisorbed oxygen denoted by O_{II} in Figure 4d. Therefore, the surface oxygen (O₂) absorbed capacity was significantly enhanced and improved reacting with the target gas species that resulted in the attainment of a high gas response as a sensing material [21].

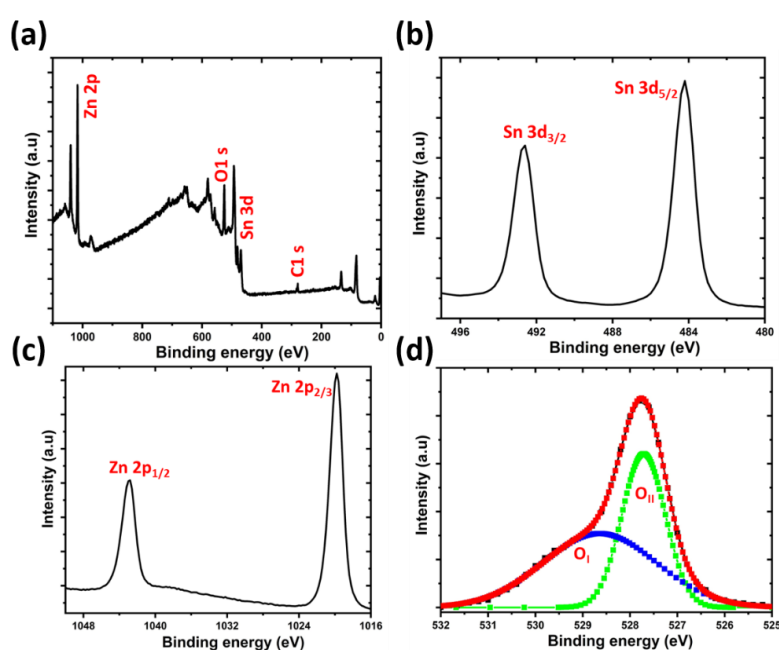


Figure 4. XPS spectrum and the fitted data; (a) full survey scan XPS spectrum of SnO₂/ZnO heterostructures, (b) Sn 3d, (c) Zn 2p, (d) O 1s of SnO₂/ZnO heterostructures.

For MOS gas sensors, operating temperature plays a dynamic role in determining the gas response of gas sensor. It is because of the dependence of desorption, and adsorption procedures of O₂ molecules takes place on the surface of the sensor [22]. Hence, first we examined the gas response of pure SnO₂, ZnO, and SnO₂/ZnO heterostructure samples towards NO₂ gas at various operating temperatures fluctuating from 25–400 °C, and the result is presented in Figure 5a. The gas response is increased in all the three cases, reached to the maximum value and then rapidly decreased. The optimum operating temperature was about 100 °C, as can be seen in the Figure 5a. Moreover, compared to their mono-counterparts the SnO₂/ZnO exhibits about a six times higher gas response towards NO₂ gas. The enhanced gas response in the instance of SnO₂/ZnO may be credited to the formation of heterostructures. At lower working temperatures gas kinetics is low and results in a lower sensor response. Similarly, at higher working temperatures, more than optimal working temperature, the kinetics of gas species more than that of molecules, might seepage from their active sites of the surface, formerly the reaction, and would disturb the amount of adsorbed gas. Henceforth, they are subsequent in a low sensor response. At optimal working temperature (100 °C) the sensor response is higher which might be because of more surface interactions and oxygen vacancies. The consequences also display the outcome of crystallinity reliant on sensing performances for thin-film gas sensors

wherever higher crystallinity achieves an enhanced sensor response. The dynamic gas response of the SnO₂/ZnO heterostructures sensor to various NO₂ concentrations varies from 5–50 ppm, as displayed in Figure 5b. The gas response is increased with a rise in NO₂ gas concentration. The sensor exhibits a noticeable gas response from 26.4 towards 5 ppm NO₂ with very rapid response-recovery times of around 20 s and 45 s, respectively.

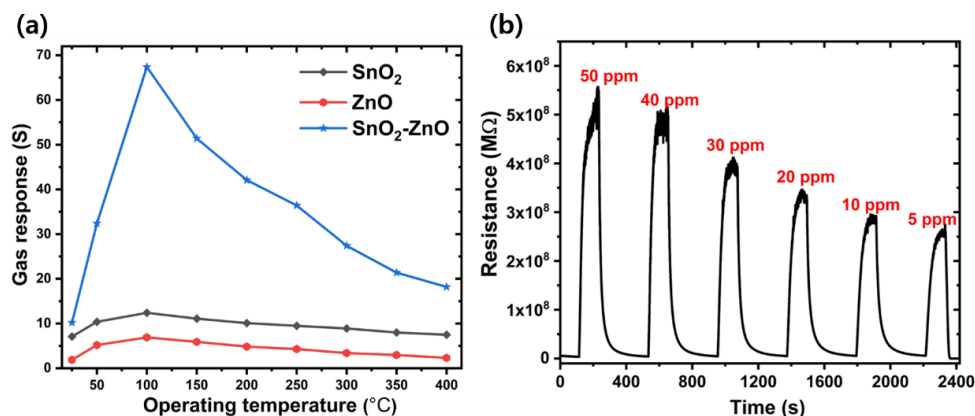


Figure 5. (a) Evaluation of gas response for SnO₂, ZnO, and SnO₂/ZnO heterostructures at various operating temperatures, (b) response curves of SnO₂/ZnO heterostructures towards NO₂ concentration of 5–50 ppm.

Figure 6a displays the reproducibility test of the SnO₂/ZnO sensor by measuring the gas response for five successive cycles after the insertion to NO₂ gas at even intermissions. It is clear from Figure 6a, that the SnO₂/ZnO sensor exhibits variation in resistance from R_a to R_g after insertion and injection to NO₂ gas; the sensor recovers its initial value R_a from R_g. This result shows excellent reproducibility of the SnO₂/ZnO sensor. Selectivity is a significant factor to study gas sensing performance of the gas sensor. Hence, for the practical opinion of application, the gas sensor must present high selectivity. Thus, a superior consideration has been given in this study, to the cautious valuation of selectivity of the sensor. The SnO₂/ZnO heterostructure sensor is examined by measuring numerous interfering gases such as acetone, hydrogen, methanol, ammonia, and ethanol at 100 °C towards 100 ppm NO₂ gas. The sensor displays low gas response to other interfering gases excluding NO₂, signifying its high specific adsorption capability towards NO₂, as revealed in Figure 6b. High gas response to NO₂ is credited to its high electron-withdrawing ability, in comparison to other interfering gases.

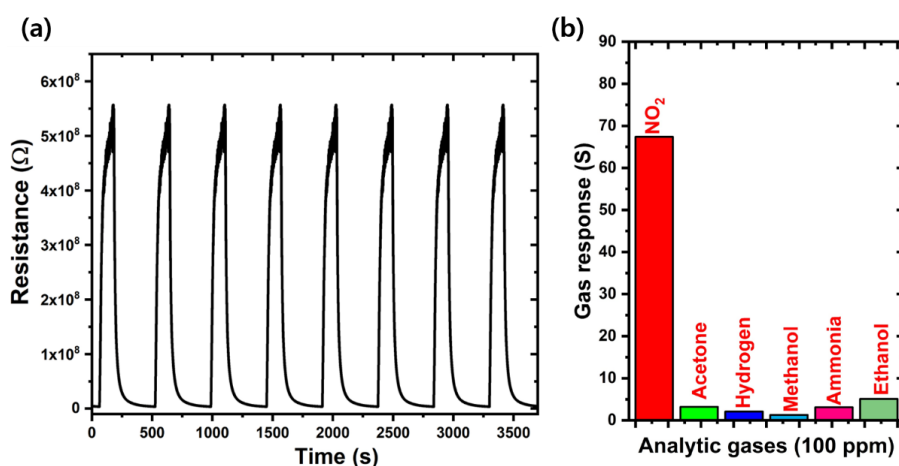


Figure 6. (a) Eight cycles of response–recovery curves towards 50 ppm NO₂ at the operating temperature of 100 °C, (b) selectivity measurements of SnO₂/ZnO heterostructures towards various test gases with concentrations of 100 ppm.

The sensing mechanism of n-type MOS sensors have been studied through the space-charge layer method [23,24]. The electrical resistance of MOS will vary after being exposed to various oxidizing or reducing gases. In air, O₂ molecules can adsorb onto the surface that leads to surface adsorbed O₂ species (O⁻_(ads), O⁻²_(ads), O²⁻_(ads)) by taking free e⁻ from the conduction band (CB). The reactions are defined as in Equations (1)–(4).



During the process, a wide e⁻ depletion layer is formed that results in the decrement of the charge carrier concentration and the rise in the electrical resistance of the sensor. After exposure to the target gas, adsorbed O₂ species react to target gas molecules. This results in e⁻ trapped in O₂ species that are sent back to CB that leads to an increase in the width of the depletion layer and a rise in the electrical resistance of the as-prepared sensor. According to literature, selectivity of the sensor depends on the many aspects like the lowest unoccupied molecules orbit (LUMO) energy of target gas molecules and the adsorption of the gas molecules onto the surface of sensing materials at various operating temperatures. In addition, electron affinity can be changed by the orbital energy of the target gas molecules. The smaller the LUMO energies the higher the gas molecules' capability to capture electrons. Thus, at an operating of temperature 100 °C, LUMO energy of NO₂ is lesser compared to other interfering gases, the capability of taking e⁻ of NO₂ will be sturdier compared to other interfering gases, and hence the sensor displays a high gas response towards NO₂ gas [25].

These results exhibited that SnO₂/ZnO heterostructures have better gas response compared to their mono counterparts. The improvement in gas response for SnO₂/ZnO heterostructures can be credited to subsequent features. At first, the surface of SnO₂/ZnO heterostructures leads to both oxides being highly available for adsorption of the O₂ species, resulting in the creation of a depletion layer onto the surface. Thus, synergetic effects of the oxides perhaps donate the improvement of the gas response in comparison to their mono counterparts. Then, work functions of SnO₂ and ZnO that have stated 4.9 eV and 5.2 eV, respectively, results in the formation of heterojunctions among SnO₂ and ZnO [26]. Shown in Figure 7, is the schematic of energy band diagrams of the SnO₂/ZnO heterojunction in dry air and NO₂ gas. The flow of electrons form SnO₂ to ZnO till the fermi levels (FE) are balanced. This generates an e⁻ depletion layer onto the ZnO and bend SnO₂ energy band that results in a change in electrical resistance of SnO₂/ZnO heterostructures. As a sensor was exposed to NO₂ gas at the optimal operating temperature, trapped e⁻ were sent back to the CB of SnO₂/ZnO heterostructures because of the reaction between adsorbed O₂ species and NO₂ molecules. Therefore, electrical resistance of SnO₂/ZnO heterostructures was highly increased resulting in an enhanced gas response.

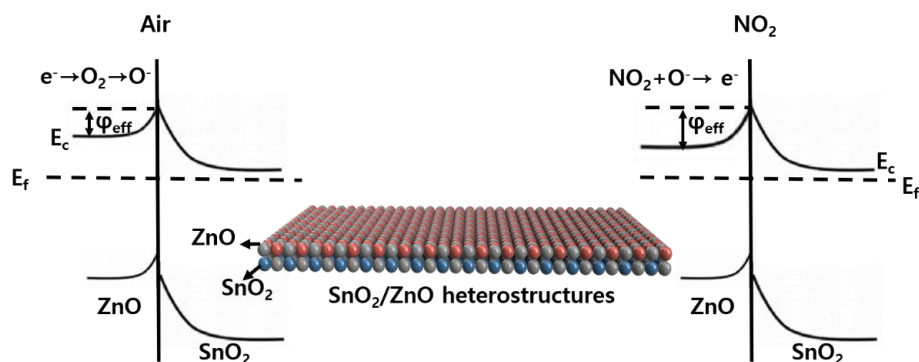


Figure 7. Schematic for energy band diagrams of SnO₂/ZnO heterostructures in dry air and NO₂.

4. Conclusions

In conclusion, the NO₂ sensors formed by SnO₂/ZnO heterostructures were fabricated and examined in this work. The morphological and structural characteristics of the SnO₂/ZnO heterostructures are identified by numerous characterization techniques. The results for SnO₂/ZnO heterostructures showed outstanding NO₂ sensing characteristics. The main reason for high gas performance was due to the SnO₂ and ZnO establishing N–N heterojunctions that significantly rise the electrical resistance of the sensor compared to pure SnO₂ and ZnO. This may be the foremost cause for the improved gas response towards NO₂. Our study offers a balanced method for the fabrication and design of resistive gas sensors with enhanced sensing characteristics.

Author Contributions: B.S. (Writing—original draft, Writing—review and editing, Methodology, Validation, Supervision); A.S. (Writing—review and editing, Investigation); M.J. (Investigation, Validation, Writing—review and editing); J.-h.M. (Formal analysis, Writing—original draft, Writing—review and editing, Project administration). All authors have read and agreed to the published version of the manuscript.

Funding: This research was funded by National Research Foundation of Korea, grant number NRF-2018R1C1B5044487 and NRF-2019K1A3A1A16106193” and “The APC was funded by NRF-2019K1A3A1A16106193.

Acknowledgments: This work was supported by National Research Foundation of Korea (NRF-2018R1C1B5044487 and NRF-2019K1A3A1A16106193).

Conflicts of Interest: The authors declare no conflict of interest.

References

1. Shendage, S.S.; Patil, V.L.; Vanalakar, S.A.; Patil, S.P.; Harale, N.S.; Bhosale, J.L.; Kim, J.H.; Patil, P.S. Sensitive and selective NO₂ gas sensor based on WO₃ nanoplates. *Sens. Actuators B Chem.* **2017**, *240*, 426–433. [[CrossRef](#)]
2. Sharma, B.; Myung, J.H. Enhanced nitrogen dioxide sensing properties of Ni₄Cr₁/SnO₂ heterostructures. *Ceram. Int.* **2020**, *46*, 19311–19317. [[CrossRef](#)]
3. Sharma, B.; Sharma, A.; Kim, J.S. Recent advances on H₂ sensor technologies based on MOX and FET devices: A review. *Sens. Actuators B Chem.* **2018**, *262*, 758–770. [[CrossRef](#)]
4. Dey, A. Semiconductor metal oxide gas sensors: A review. *Mater. Sci. Eng. B* **2018**, *229*, 206–217. [[CrossRef](#)]
5. Zhang, Z.; Wen, Z.; Ye, Z.; Zhu, L. Ultrasensitive ppb-level NO₂ gas sensor based on WO₃ hollow nanosphers doped with Fe. *Appl. Surf. Sci.* **2018**, *434*, 891–897. [[CrossRef](#)]
6. Han, D.; Zhai, L.; Gu, F.; Wang, Z. Highly sensitive NO₂ gas sensor of ppb-level detection based on In₂O₃ nanobricks at low temperature. *Sens. Actuators B Chem.* **2018**, *262*, 655–663. [[CrossRef](#)]
7. Gawali, S.R.; Patil, V.L.; Deonikar, V.G.; Patil, S.S.; Patil, D.R.; Patil, P.S.; Pant, J. Ce doped NiO nanoparticles as selective NO₂ gas sensor. *J. Phys. Chem. Solids* **2018**, *114*, 28–35. [[CrossRef](#)]
8. Patil, V.L.; Vanalakar, S.A.; Patil, P.S.; Kim, J.H. Fabrication of nanostructured ZnO thin films based NO₂ gas sensor via SILAR technique. *Sens. Actuators B Chem.* **2017**, *239*, 1185–1193. [[CrossRef](#)]
9. Ponzoni, A.; Baratto, C.; Cattabiani, N.; Falasconi, M.; Galstyan, V.; Nunez-Carmona, E.; Rigoni, F.; Sberveglieri, V.; Zambotti, G.; Zappa, D. Metal oxide gas sensors, a survey of selectivity issues addressed at the SENSOR Lab, Brescia (Italy). *Sensors* **2017**, *17*, 714. [[CrossRef](#)]
10. Walker, J.M.; Akbar, S.A.; Morris, P.A. Synergistic effects in gas sensing semiconducting oxide nano-heterostructures: A review. *Sens. Actuators B Chem.* **2019**, *286*, 624–640. [[CrossRef](#)]
11. Shan, H.; Liu, C.; Liu, L.; Zhang, J.; Li, H.; Liu, Z.; Zhang, X.; Bo, X.; Chi, X. Excellent toluene sensing properties of SnO₂–Fe₂O₃ interconnected nanotubes. *ACS Appl. Mater. Interfaces* **2013**, *5*, 6376–6380. [[CrossRef](#)] [[PubMed](#)]
12. Yan, S.; Ma, S.; Xu, X.; Lu, Y.; Bian, H.; Liang, X.; Jin, W.; Yang, H. Synthesis and gas sensing application of porous CeO₂–ZnO hollow fibers using cotton as biotemplates. *Mater. Lett.* **2016**, *165*, 9–13. [[CrossRef](#)]
13. Lin, C.Y.; Fang, Y.Y.; Lin, C.W.; Tunney, J.J.; Ho, K.C. Fabrication of NO_x gas sensors using In₂O₃–ZnO composite films. *Sens. Actuators B* **2010**, *146*, 28–34. [[CrossRef](#)]
14. Zhang, Z.; Xu, M.; Liu, L.; Ruan, X.; Yan, J.; Zhao, W.; Yun, J.; Wang, Y.; Qin, S.; Zhang, T. Novel SnO₂@ZnO hierarchical nanostructures for highly sensitive and selective NO₂ gas sensing. *Sens. Actuators B Chem.* **2018**, *257*, 714–727. [[CrossRef](#)]

15. Yang, X.; Zhang, S.; Zhao, L.; Sun, P.; Wang, T.; Liu, F.; Yan, X.; Gao, Y.; Liang, X.; Zhang, S.; et al. One step synthesis of branched SnO₂/ZnO heterostructures and their enhanced gas-sensing properties. *Sens. Actuators B Chem.* **2019**, *281*, 415–423. [[CrossRef](#)]
16. Vomiero, A.; Bianchi, S.; Comini, E.; Faglia, G.; Ferroni, M.; Poli, N.; Sberveglieri, G. In₂O₃ nanowires for gas sensors: Morphology and sensing characterisation. *Thin Solid Films* **2007**, *515*, 8356–8359. [[CrossRef](#)]
17. Haridas, D.; Gupta, V. Enhanced response characteristics of SnO₂-ZnO heterostructures loaded with nanoscale catalyst clusters for methane gas detection. *MRS Proc.* **2012**, *1454*, 227–232. [[CrossRef](#)]
18. Le, D.T.T.; Chinh, N.D.; Binh, B.T.T.; Hong, H.S.; Van Duy, N.; Hoa, N.D.; Van Hieu, N. Facile synthesis of SnO₂-ZnO core-shell nanowires for enhanced ethanol-sensing performance. *Curr. Appl Phys.* **2013**, *13*, 1637–1642.
19. Chen, S.; Liu, F.; Xu, M.; Yan, J.; Zhang, F.; Zhao, W.; Zhang, Z.; Deng, Z.; Yun, J.; Chen, R.; et al. First-principles calculations and experimental investigation on SnO₂@ ZnO heterojunction photocatalyst with enhanced photocatalytic performance. *J. Colloid Interface Sci.* **2019**, *553*, 613–621. [[CrossRef](#)]
20. Xu, M.; Yu, R.; Guo, Y.; Chen, C.; Han, Q.; Di, J.; Song, P.; Zheng, L.; Zhang, Z.; Yan, J.; et al. New strategy towards the assembly of hierarchical heterostructures of SnO₂/ZnO for NO₂ detection at a ppb level. *Inorg. Chem. Front.* **2019**, *6*, 2801–2809. [[CrossRef](#)]
21. Li, H.; Chu, S.; Ma, Q.; Li, H.; Che, Q.; Wang, J.; Wang, G.; Yang, P. Multilevel Effective Heterojunctions Based on SnO₂/ZnO 1D Fibrous Hierarchical Structure with Unique Interface Electronic Effects. *ACS Appl. Mater. Interfaces* **2019**, *11*, 31551–31561. [[CrossRef](#)] [[PubMed](#)]
22. Cai, N.N.; Wang, K.; Li, N.; Wang, T.; Xiao, Q. CuO meso-macroporous microspheres: Calcination-time-dependent gas-sensing performance. *Surf. Innov.* **2019**, *7*, 203–209. [[CrossRef](#)]
23. Li, Z.; Zhao, Q.; Fan, W.; Zhan, J. Porous SnO₂ nanospheres as sensitive gas sensors for volatile organic compounds detection. *Nanoscale* **2011**, *3*, 1646–1652. [[CrossRef](#)] [[PubMed](#)]
24. Chiu, H.C.; Yeh, C.S. Hydrothermal synthesis of SnO₂ nanoparticles and their gas-sensing of alcohol. *J. Phys. Chem. C* **2007**, *111*, 7256–7259. [[CrossRef](#)]
25. Chi, X.; Liu, C.; Liu, L.; Li, Y.; Wang, Z.; Bo, X.; Liu, L.; Su, C. Tungsten trioxide nanotubes with high sensitive and selective properties to acetone. *Sens. Actuators B Chem.* **2014**, *194*, 33–37. [[CrossRef](#)]
26. Dong, Z.; Kong, X.; Wu, Y.; Zhang, J.; Chen, Y. High-sensitive room-temperature NO₂ sensor based on a soluble n-type phthalocyanine semiconductor. *Inorg. Chem. Commun.* **2017**, *77*, 18–22. [[CrossRef](#)]



© 2020 by the authors. Licensee MDPI, Basel, Switzerland. This article is an open access article distributed under the terms and conditions of the Creative Commons Attribution (CC BY) license (<http://creativecommons.org/licenses/by/4.0/>).